

The Spread of the Hunga Tonga H₂O Plume in the Middle Atmosphere Over the First Two Years Since Eruption

¹Gerald E. Nedoluha, ¹R. Michael Gomez, ²Ian Boyd, ²Helen Neal, ¹Douglas R. Allen, and ³Alyn Lambert

¹Naval Research Laboratory, Washington, DC, USA

²Bryan Scientific Consulting LLC, Charlottesville, VA, USA

³Jet Propulsion Laboratory, California Institute of Technology, Pasadena, CA, USA

Corresponding author: Gerald Nedoluha (nedoluha@nrl.navy.mil)

Key Points:

- Three ground-based instruments confirm the MLS observation of a >1ppmv increase in H₂O in the lower mesosphere in 2023.
- The MLS H₂O monthly zonal anomaly from 76S-76N and 83-0.1 hPa has, for at least a month, been larger than at any time before the eruption.
- Almost all of the mass of H₂O injected into the stratosphere remains in either the stratosphere or mesosphere 22 months after the eruption.

Abstract

The eruption of Hunga Tonga in January 2022 injected a large amount of water into the stratosphere. Satellite measurements from Aura Microwave Limb Sounder (MLS) show that this water vapor (H₂O) has now spread throughout the stratosphere and into the lower mesosphere, resulting in an increase of >1 ppmv throughout most of this region. Measurements from three ground-based Water Vapor Millimeter Wave Spectrometer (WVMS) instruments and MLS are in good agreement, and show that in 2023 there was more H₂O in the lower mesosphere than at any time since the WVMS measurements began in the 1990's. At Table Mountain, California all WVMS H₂O measurements at 54 km since June 2023, and all of the measurements from Mauna Loa, Hawaii, since the resumption of measurements in September 2023, show larger mixing ratios than any previous measurements. At 70 km several recent ~1 week WVMS retrievals in the last few months show the largest anomalies ever measured. The MLS measurements show that maximum H₂O anomalies have occurred throughout almost all of the stratosphere and lower mesosphere since the eruption. As of November 2023, almost all of the ~140 Tg of water originally injected into the stratosphere by the Hunga Tonga eruption remains in the middle atmosphere at pressures below 83 hPa (altitudes above ~17 km). The eruption occurred during a period when stratospheric H₂O was already slightly elevated above the 2004-2021 MLS average, and the November 2023 anomaly of ~160 Tg represents ~15% of the total mass of H₂O in this region.

Plain Language Summary

The eruption of the undersea Hunga Tonga volcano on 15 January 2022 injected large amounts of water vapor into the stratosphere, breaking all records for direct injection of water vapor

42 (H₂O) in the satellite era. Water vapor mixing ratios in the stratosphere and lower mesosphere
43 (~20-65km) range from ~2-8 ppmv depending upon height, latitude, and season, and satellite
44 measurements from Aura Microwave Limb Sounder (MLS) show that this water vapor has now
45 spread throughout the stratosphere and into the lower mesosphere, resulting in an increase of >1
46 ppmv nearly globally throughout this altitude range. The MLS measurements are confirmed at
47 three sites by the ground-based Water Vapor Millimeter Wave Spectrometer (WVMS)
48 instruments, and all of these measurements show that there is more H₂O in the lower mesosphere
49 (~50-65km) than at any time since the WVMS measurements began in the 1990's. At 70 km
50 several WVMS measurements in the last few months show the largest anomalies ever measured.
51 As of November 2023, almost all of the ~140 Tg of water originally injected into the
52 stratosphere by the Hunga Tonga eruption remains in the middle atmosphere at pressures below
53 83 hPa (altitudes above ~17 km).

54 **1 Introduction**

55 On 15 January 2022, the eruption of the Hunga Tonga undersea volcano injected huge amounts
56 of water vapor (H₂O) into the atmosphere. Measurements showed that a small amount of this
57 H₂O was injected directly into the lower mesosphere (Millan et al., 2022; Carr et al., 2022);
58 however, a much larger quantity was injected into the stratosphere. The early evolution of this
59 stratospheric H₂O plume has been documented in several studies (Millan et al., 2022; Legras et
60 al., 2022; Khaykin et al., 2022; Schoeberl et al., 2022; Nedoluha et al., 2023a). Fleming et al.
61 (2024) have presented some calculations of the effect of this additional H₂O on O₃ and
62 temperature over the next decade.

63 Nedoluha et al. (2023b) (hereafter N23) documented an increase in mesospheric H₂O in 2022.
64 Measurements from MLS and three ground-based microwave instruments often recorded the
65 highest H₂O mixing ratio anomalies ever seen. N23 concluded that a portion of this increase was
66 caused by some of the H₂O-enriched air from Hunga Tonga that had risen slowly through the
67 stratosphere and into the lower mesosphere. But it was also noted that the observed H₂O
68 increases in 2022 in the lower mesosphere were caused, at least in part, by dynamical conditions
69 that allowed for an anomalous amount of methane (CH₄) oxidation.

70 In this study we document the further spread of the Hunga Tonga H₂O plume in the stratosphere
71 and the increase in mesospheric H₂O observed in 2023. While the high mesospheric H₂O mixing
72 ratios observed in 2022 were unprecedented, the increase observed in 2023 was much larger and
73 more widespread. We also document the timescales over which the injected H₂O mass spread
74 throughout the middle atmosphere from the January 2022 eruption until November 2023.

75 **2. Ground-based and Satellite Datasets**

76 The WVMS instruments have been making nearly continuous measurements of H₂O in the
77 middle atmosphere since the early 1990's. Measurements are made from the Network for the
78 Detection of Atmospheric Composition Change (NDACC) sites at Table Mountain, California
79 (34.4° N, 242.3° E), Mauna Loa, Hawaii (19.5° N, 204.4° E), and Lauder, New Zealand (45.0° S,
80 169.7° E). These instruments make spectrally resolved measurements of the 22 GHz H₂O
81 emission line to obtain a vertical profile of H₂O. The vertical resolution in the mesosphere is
82 ~16 km (FWHM).

83 The standard WVMS measurement product, which will be used in this study, is retrieved from a
84 ~1 week integration of the spectrum within +/-30 MHz of the H₂O emission peak at 22 GHz.
85 The precise time period is determined by variations in conditions at each site. Results from these
86 retrievals from 1992 to 2021 were presented in Nedoluha et al. (2022), where H₂O vertical
87 profiles were shown from 45 km to 80 km.

88 The measurements from Mauna Loa were interrupted on 27 November 2022, by a lava flow
89 which cut power, communications, and road access to the site. Solar panels were flown in and
90 installed by helicopter in September 2023, and these provide sufficient power to operate a single
91 WVMS instrument. The WVMS6, which had been providing the long-term dataset was initially
92 brought back into operation, but the initial performance was unsatisfactory. Since 26 September
93 2023 the H₂O measurements are therefore being made with the WVMS5 instrument, which had
94 previously been used primarily for experimentation and to validate WVMS6 measurements. The
95 WVMS5 instruments makes use of a new corrugated gaussian horn antenna design developed
96 specifically for WVMS5 by Dr. Jorge Teniente and the Antenal Antenna group (Teniente et al.,
97 2011]. This antenna went through many years of development on WVMS5 to improve the
98 reflectivity (S11) and the H and E plane differences in order to reduce the baseline created by the
99 use of both antenna planes and an absorber bar in the signal-reference measurement (Gomez et
100 al., 2012).

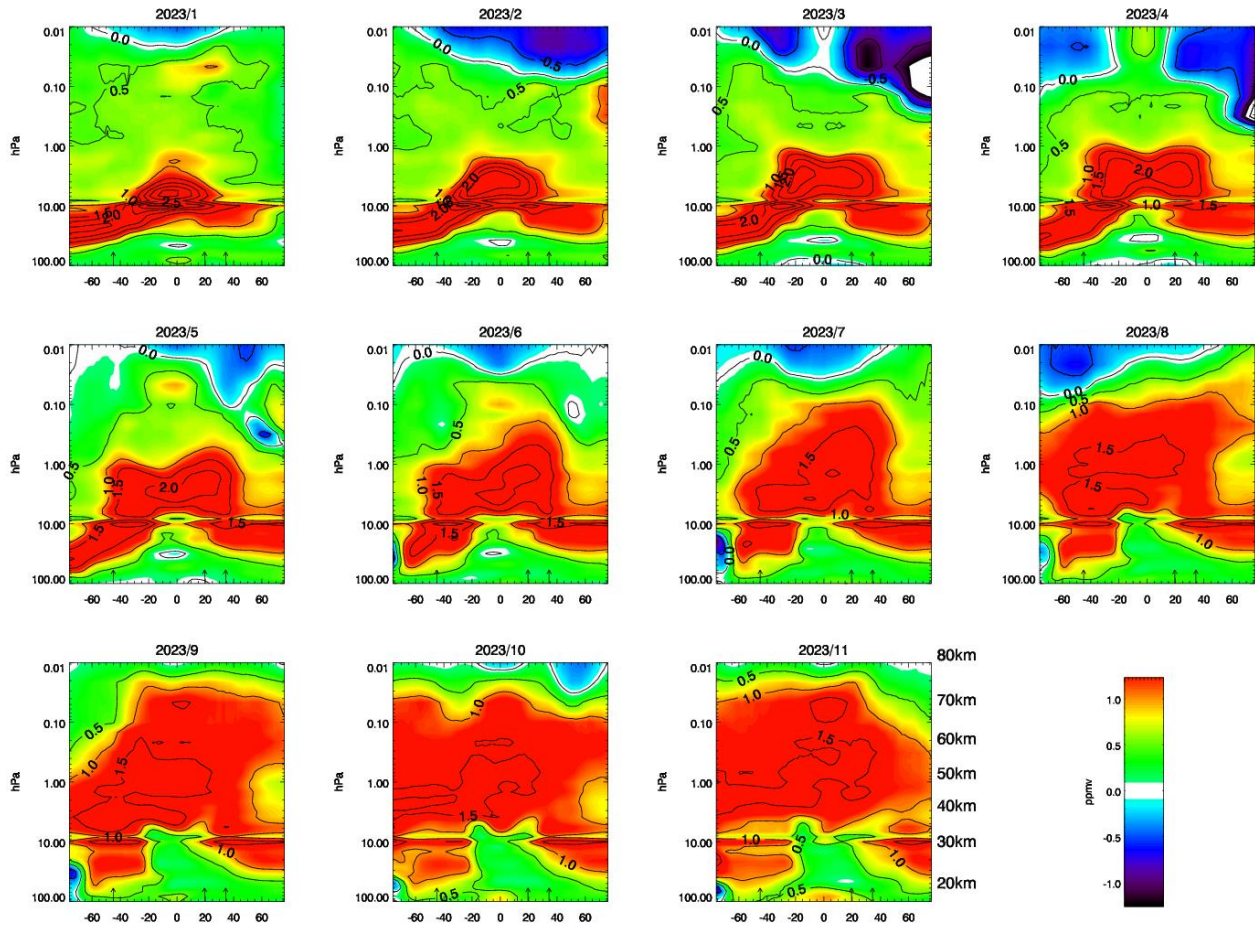
101 There has been a slight adjustment to the WVMS H₂O retrievals from Lauder that are presented
102 here relative to those shown in N23 which particularly affected the H₂O mixing ratios in July and
103 August 2022. The WVMS retrievals rely upon a background temperature, and in N23 the
104 temperatures for that period were calculated using an MLS climatology of coincident
105 measurements covering the days of the ~1 week WVMS retrieval. Here we have made use of the
106 average of the contemporaneous MLS temperatures taken during the ~1 week WVMS. The
107 difference between climatological and measured temperature is usually small, however the year-
108 to-year mesospheric temperatures near Lauder from June through August are particularly
109 variable. In 2022 these differed by >10K from climatology over several weeks. An incorrect
110 temperature background of 10K causes an error in the retrieved H₂O of ~0.5 ppmv in the
111 mesosphere, and the new WVMS retrievals show variations that are in slightly better agreement
112 with MLS.

113 The Aura MLS H₂O product is retrieved from the radiances measured by the radiometers
114 centered near 190 GHz. The MLS v4 H₂O retrievals were used in Millan et al. (2022) because of
115 poor fits in v5 retrievals in regions of extremely enhanced H₂O. In this study we use v5
116 retrievals, but, except in direct comparisons with WVMS measurements, we show monthly zonal
117 medians in order to limit the effect of any problems with MLS measurements when the H₂O
118 values are extremely enhanced. The v5 retrievals are generally recommended by the MLS Team.
119 Livesey et al. (2021) showed that the v5 retrievals remove an upward drift in the MLS v4 H₂O
120 measurements of ~2-4%/decade from ~50 hPa to 0.1 hPa since 2010 relative to the Atmospheric
121 Chemistry Experiment Fourier Transform Spectrometer (ACE-FTS) (Bernath, et al., 2005).
122 Those profile comparisons showed a kink in the relative drift near 10 hPa, a feature that is
123 apparent in plots showing MLS H₂O anomalies relative to climatology near this level.

124 To compare with H₂O variations in the 1990's we also show observations from the Halogen
125 Occultation Experiment (HALOE). HALOE observed between 2.45 and 10.0 μm using a solar
126 occultation technique which provided measurements in two separate latitude bands on any day
127 (one in sunrise mode and one in sunset mode). A full description of the design and operation is
128 given by Russell et al. (1993). The results shown here use the HALOE third public release v19
129 retrievals.

130 **3. WVMS, MLS, and HALOE Measurements of H₂O**

131 In Figure 1 we show the monthly zonal median H₂O mixing ratio anomalies in the stratosphere
132 and mesosphere for January to November, 2023. The anomalies are calculated relative to a
133 2004-2021 MLS-based climatology. The year begins with positive anomalies almost
134 everywhere, with the largest anomalies in the lower stratosphere and in the tropical upper
135 stratosphere. From January through April the strong tropical anomalies spread both northwards
136 and southwards in the upper stratosphere. During this period the anomaly in the tropical lower
137 stratosphere decreases as younger stratospheric air, unperturbed by the Hunga Tonga eruption,
138 rises through the tropopause. Then, in June 2023 mixing ratio anomalies >1 ppmv spread into
139 the northern midlatitude lower mesosphere (~ 1 hPa to 0.1 hPa). By August, the lower
140 mesosphere from ~50S to 50N shows anomalies > 1 ppmv, with actual mixing ratios >8 ppmv
141 throughout most of this region. In October 2023, almost the entire upper stratosphere (10 to 1
142 hPa) and lower mesosphere shows anomalies > 1 ppmv, with the sole exception being the
143 Northern Hemisphere (NH) upper stratosphere.

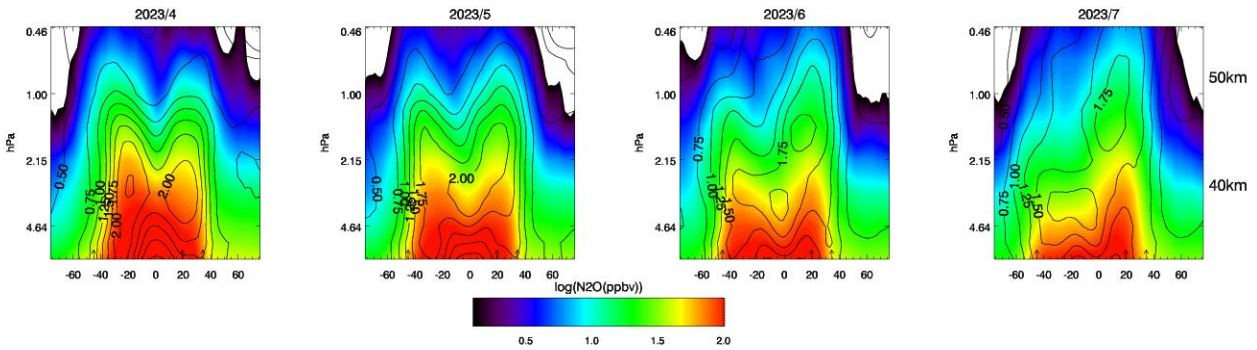


144

145 **Figure 1**– The monthly zonal-median H₂O anomaly relative to a 2004-2021 MLS climatology
 146 for MLS measurements from January to November 2023 for latitudes 75°S to 75°N. Data is
 147 shown on the native MLS pressure levels. Indicated altitudes are approximate. The arrows
 148 indicate the latitudes of the WVMS sites. Contours are in 0.5 ppmv intervals up to 2 ppmv, and
 149 in 1 ppmv intervals for larger H₂O mixing ratio anomalies.

150 In Figure 2 we show MLS nitrous oxide (N₂O) measurements (not anomalies) with contours of
 151 H₂O anomalies superimposed. Like N₂O, CH₄ has a sharply decreasing vertical gradient in the
 152 upper stratosphere, and CH₄ measurements from the HALOE instrument in the early 1990’s
 153 showed a similar “rabbit ear” structure in latitudinal variation in April (Randel et al., 1998).
 154 High N₂O values are indicative of younger air, and Figure 2 shows that in 2023 this rising
 155 younger air brings with it H₂O-enriched air from the Hunga Tonga plume. In April both the H₂O
 156 anomaly and the N₂O mixing ratios in the upper stratosphere are slightly higher in the Southern
 157 Hemisphere (SH) than NH midlatitudes. From May through June, with the beginning of Boreal
 158 summer, this hemispheric asymmetry is reversed, and the H₂O anomalies >1.75 ppmv begin to
 159 enter the NH lower mesosphere.

160



161

162 **Figure 2-** The monthly zonal-median N_2O mixing ratios (colors) and H_2O mixing ratio
 163 anomalies (lines) as measured by MLS from April through July 2023 for 75°S to 75°N . The
 164 indicated altitudes are approximate.

165 In Figure 3 we show WVMS and coincident MLS H_2O measurements near the WVMS sites
 166 from January 2022 through November 2023. The MLS measurements are an average over a
 167 coincident time period (usually ~ 1 week) within $\pm 2^\circ$ latitude, $\pm 30^\circ$ longitude of the WVMS sites,
 168 and are convolved with WVMS averaging kernels appropriate to each site (e.g., Nedoluha et al.,
 169 2022). The H_2O increase at 54 km is first observed at Table Mountain and Mauna Loa, and then
 170 slightly later at Lauder.

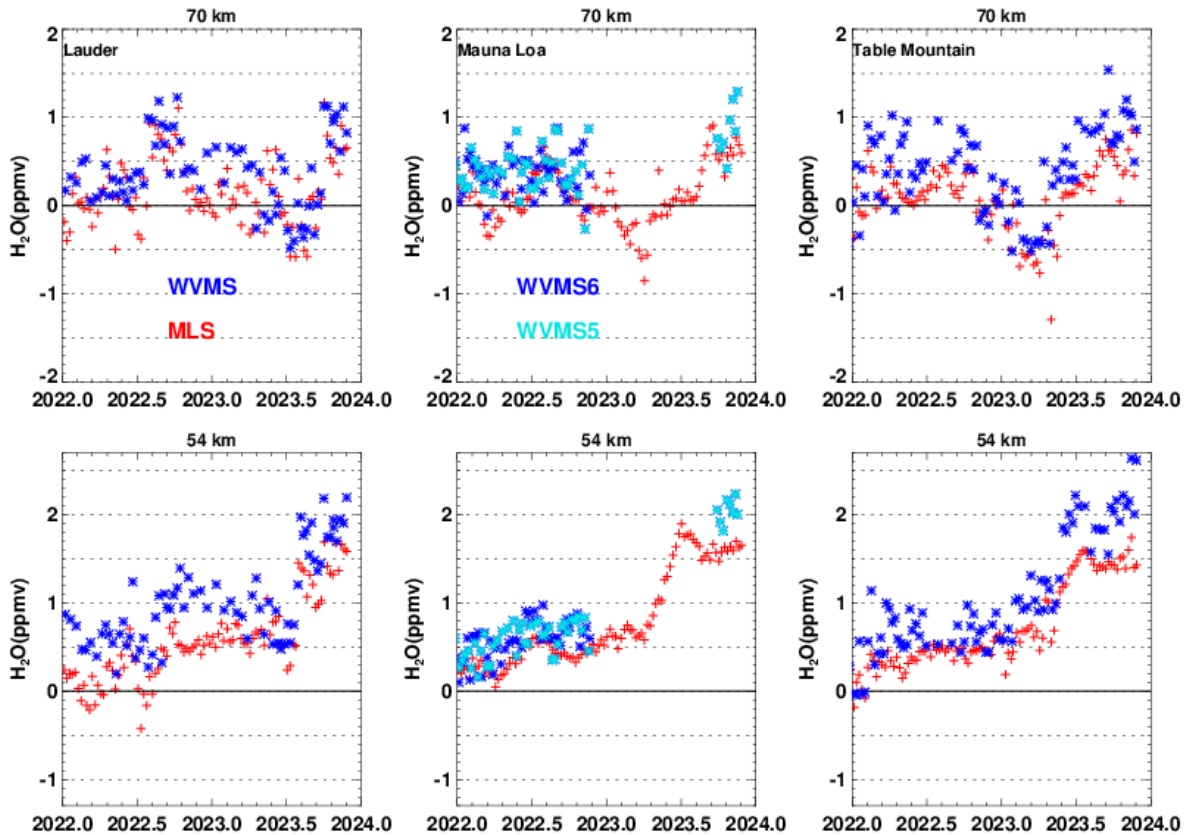
171 The gap in the WVMS data from Mauna Loa is the result of the cut in power and
 172 communications caused by the eruption of Mauna Loa. As noted in Section 2, there are two
 173 WVMS instruments at Mauna Loa, with the primary timeseries provided by the WVMS6
 174 instrument. However, since there was some difficulty with the restart of WVMS6, and since the
 175 solar panels only provide sufficient power for one instrument, the post-Mauna Loa eruption
 176 measurements are currently being provided by WVMS5. Before the Mauna Loa eruption
 177 WVMS5 and WVMS6 were in good agreement, as can be seen in Figure 3.

178 Figure 3 shows the large mid-2023 increase in H_2O in the lower mesosphere observed by
 179 WVMS and coincident MLS measurements at Lauder, Mauna Loa, and Table Mountain. Some
 180 of the WVMS measurements are biased slightly high relative to the MLS measurements, but the
 181 magnitude of the observed increase in lower mesospheric H_2O is in good agreement. As was
 182 noted in N23 the H_2O mixing ratios at 54 km were already at record-high levels by the end of
 183 2022. However, based on an analysis of coincident N_2O measurements and the phase of quasi-
 184 biennial oscillation (QBO), it was shown that a significant component of the observed increase in
 185 the lower mesosphere was probably caused by dynamical variations (slower ascent) unrelated to
 186 Hunga Tonga. In 2023, however, there was a much larger increase in lower mesospheric H_2O ,
 187 and the MLS N_2O measurements do not indicate that this is a period of unusually slow ascent
 188 that would lead to an increase in H_2O . This increase can therefore only be ascribed to the Hunga
 189 Tonga plume.

190 The H_2O anomalies at 70 km in Figure 3 also show an increase throughout much of 2023, but
 191 dynamical variations cause much larger anomaly variations at this altitude than in the lower
 192 mesosphere. As was noted in N23, the large increase in anomalous H_2O mixing ratio observed

193 over Lauder in 2022 was coincident with a large decrease in anomalous carbon monoxide (CO).
194 Similar variations in H₂O and CO occurred in 2015 during a similar phase of the QBO. N23
195 therefore concluded that a significant portion of the 2022 upper mesospheric increase over
196 Lauder was probably not caused by Hunga Tonga.

197 In late 2022 there was a decrease in H₂O at 70 km at both Mauna Loa and Table Mountain,
198 followed in subsequent months by an increase of comparable magnitude. At Lauder there was a
199 sharp increase in 70 km H₂O at the end of 2023. The two measurements of H₂O anomalies >1
200 ppmv at 70 km at Mauna Loa in November 2023 are the only such measurements since those
201 WVMS observations began in 1996. Similarly, the 16-23 September 2023 WVMS
202 measurements at Table Mountain which shows an anomaly of >1.5 ppmv is the only such
203 measurement since observations began in 1992, while the second largest anomaly (1.2 ppmv)
204 occurred during the 31 October to 6 November 2023 retrieval. Thus, the MLS and WVMS
205 measurements suggest that increase H₂O from Hunga Tonga is affecting H₂O values in the upper
206 mesosphere as well. This increase in H₂O occurs during a period when solar irradiance is
207 increasing and thus causing increased photodissociation of H₂O (and hence lower H₂O mixing
208 ratios) in the mesosphere. The Lyman- α solar irradiance in 2023 is higher than at any time since
209 the maxima during solar cycle 23 which peaked in 2001-2002
210 (lasp.colorado.edu/lisird/data/composite_lyman_alpha).

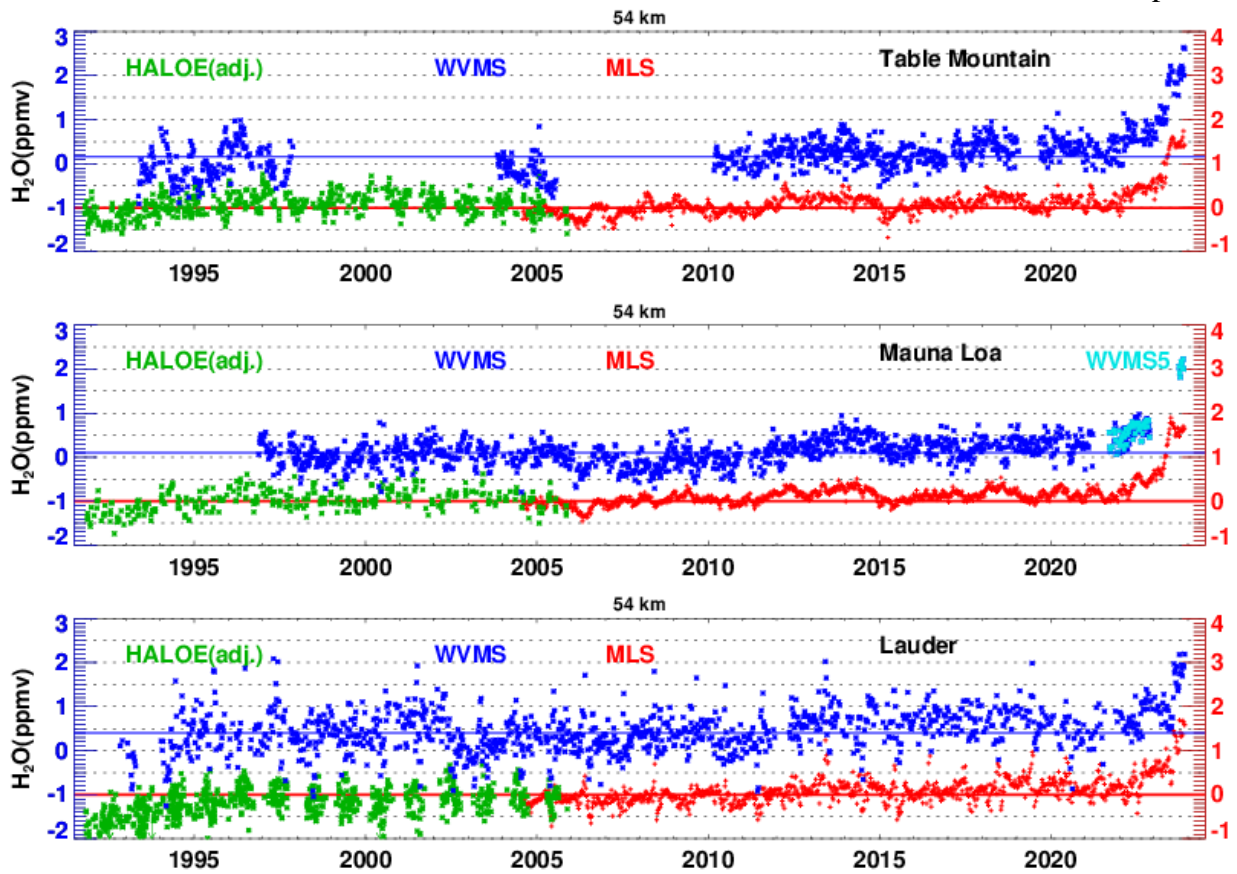


212 **Figure 3-** WVMS H₂O anomalies (blue and cyan; see text) and coincident MLS measurements
213 (red) at three WVMS sites. The MLS measurements have been convolved with WVMS
214 averaging kernels. The anomalies are calculated relative to an MLS 2004-2021 H₂O
215 climatology.

216 To put the recent lower mesospheric increase into a multidecadal context we show in Figure 4
217 the H₂O timeseries at 54 km at the three WVMS sites since 1991. At Table Mountain all of the
218 ~weekly 54 km WVMS H₂O measurements since June 2023, and all of the measurements from
219 Mauna Loa since the resumption of measurements in September 2023, show larger anomalies
220 relative to the MLS climatology, and also larger absolute mixing ratio values, than any previous
221 measurements. Near Lauder there are strong latitudinal gradients in mesospheric H₂O from June
222 through August (coincident with the temperature gradients mentioned in Section 2), and this can
223 cause a large weekly H₂O anomaly that is comparable to the increase caused by Hunga Tonga.
224 Also, the WVMS measurements from Lauder are inherently noisier due to the high tropospheric
225 opacity at the site. But the presence in both WVMS and MLS measurements of anomalies
226 consistently more than 0.9 ppmv above the instrumental average since mid-July 2023 is
227 unprecedented.

228 The timeseries shown in Figure 4 allows for comparison of the H₂O variations following the
229 Hunga Tonga eruption with the gradual increase seen in the early 1990's in measurements from
230 HALOE, and from the WVMS instruments at Lauder and Table Mountain (Evans et al.,1998;
231 Nedoluha et al., 1998a). Nedoluha et al. (2003) showed an increase of ~0.4 ppmv in upper
232 stratospheric and lower mesospheric measurements from HALOE from 1991-1995, with a
233 significant fraction of that increase driven by increased CH₄ oxidation caused by dynamical
234 variations (Nedoluha et al. 1998b). When compared to the 1990's H₂O increase near the
235 stratopause, the change in H₂O from the Hunga Tonga plume is both much larger and occurs

236 over a much shorter period.



237

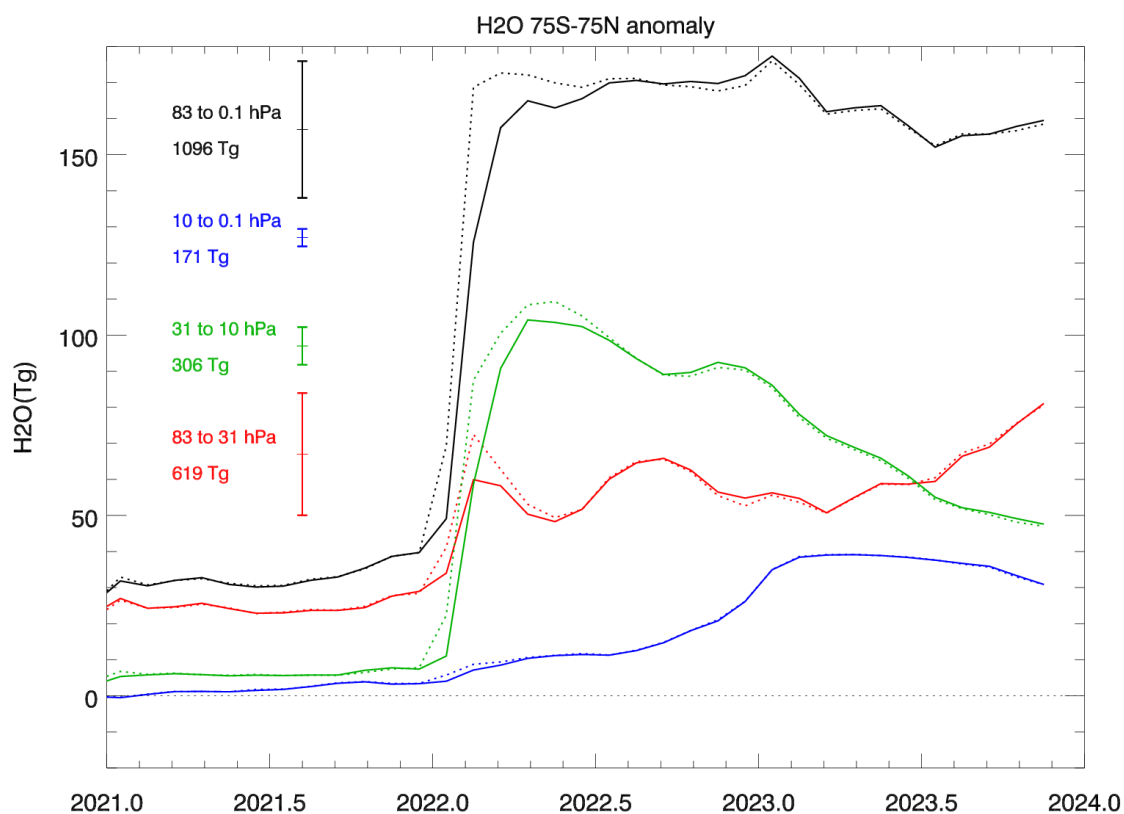
238 **Figure 4-** H₂O anomalies at 54 km from WVMS (blue and cyan; see text), HALOE (green) and
239 MLS (red) at, or coincident with, the three WVMS sites. The HALOE and MLS measurements
240 have been convolved with WVMS averaging kernels. The satellite measurements are referenced
241 to the right-hand axis which, to prevent overplotting of data, is offset by 1 ppmv from the axis
242 for the WVMS measurements. The measurements from HALOE have been adjusted to create an
243 unbiased time series relative to MLS. The blue line shows the average WVMS offset from the
244 MLS climatology.

245 4. The Spread and Persistence of the Hunga Tonga H₂O Plume

246 In Figure 5 we show the variation of the mass of H₂O in the stratosphere from 83 hPa to 0.1 hPa
247 since the beginning of 2021 (latitudes from 75°S to 75°N represent ~97% of the global area). As
248 in previous plots, the values shown are calculated from monthly zonal mixing ratio anomalies
249 from the 2004-2021 climatology, but for Figure 5 these values are integrated over the indicated
250 pressure range and area to provide a mass. The typical annual variation measured by MLS over
251 this entire pressure range and latitude region, which comes almost entirely from the lowermost
252 altitudes, is ~30-40 Tg. As was shown in Nedoluha et al. (2023a) the 365-day mean 100 hPa
253 tropopause temperature was ~0.5 K to 0.9 K above the 42-year mean in 2021. The high average
254 tropopause temperature during 2021 is probably the primary reason why the mass of H₂O in the
255 83 hPa to 31 hPa level is ~25 Tg above the 2004-2021 climatological value. The value in this
256 level in 2021 is not unusual, but is comparable to the highest levels measured since 2004.

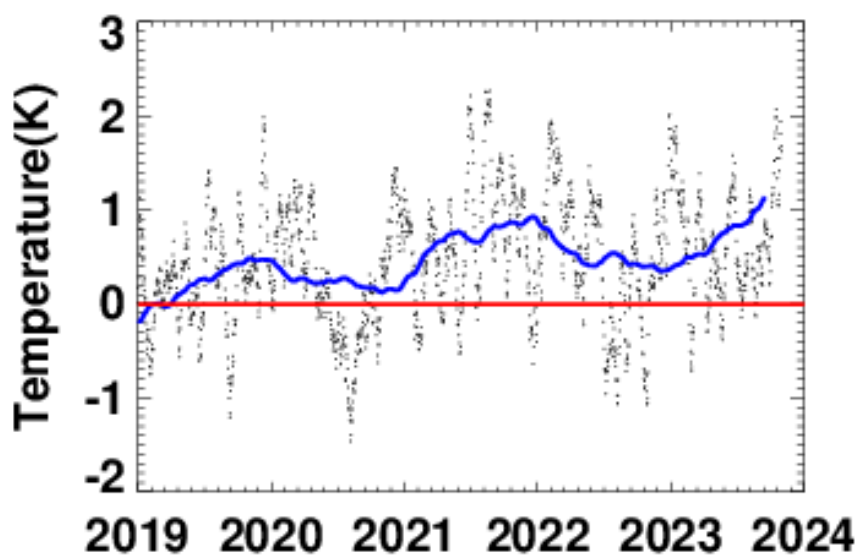
257 The average mass of H₂O from 83 hPa to 0.1 hPa and 75°S to 75°N in 2021 in the MLS
 258 measurements was 1096 Tg. Initial calculations of additional stratospheric H₂O mass from the
 259 MLS measurements range from ~130 to 150 Tg (Millan et al. (2022), Xu et al. (2022), and
 260 Khaykin et al. (2022)), consistent with the increase shown in Figure 5. Results are shown both
 261 from zonal median and zonal mean anomalies, and the results are nearly identical except in the
 262 months immediately following the eruption when the plume had not yet spread evenly over all
 263 longitudes.

264 Wilmouth et al., (2023), using 2021 as a background, found that, through the end of 2022, the
 265 global H₂O enhancement from 100 hPa to 1.2 hPa, referenced to 2021, had decreased slightly,
 266 from 145 Tg to 135 Tg. Figure 5 also shows that there has been only a slight decrease in the
 267 total amount of H₂O above 83 hPa during the almost two years after the eruption. While the
 268 anomaly in H₂O in the 31 hPa to 10 hPa region is now only ~1/2 as large as immediately after
 269 the eruption, a significant fraction of this mass has risen to altitudes with pressures below 10 hPa.



270
 271 **Figure 5**- The monthly H₂O mass anomaly from 82 hPa to 0.1 hPa as measured by MLS from
 272 75°S to 75°N. Results are shown both as calculated from the zonal median anomalies (solid) and
 273 zonal mean anomalies (dotted). The error bars indicate the standard deviation of the monthly
 274 mass anomaly over the indicated pressure ranges for MLS measurements from 2004 through
 275 January 2022. Also shown in the labels is the mean of the 2021 H₂O mass in each pressure
 276 layer.

277 The excess H₂O in the 83 to 31 hPa layer has also increased since early 2023. Figure 1 suggests
 278 that there is some increase in this layer from descending air from the Hunga Tonga plume, but
 279 about ½ of the increase since March 2023 occurs in the 20°S-20°N region, so this suggests an
 280 increase H₂O entering the stratosphere through the tropical tropopause. Dessler et al. (2014),
 281 using trajectory calculations, showed a close correlation between MLS H₂O anomalies and
 282 Modern-Era Retrospective analysis for Research and Applications (MERRA) temperatures in
 283 this region. Figure 6 shows MERRA2 temperatures at 100 hPa from 10°S-10°N. These are
 284 consistently well above the long-term average from the beginning of 2021 onwards, and there is
 285 a further increase in 2023, suggesting that some of the increase in the lower layer shown in
 286 Figure 5 is probably the result of an increase in H₂O entering the stratosphere. The H₂O anomaly
 287 above 83 hPa in November 2023 was ~160 Tg, which represents an excess of ~15% over the
 288 average amount of H₂O measured in this region by MLS from 2004-2021.



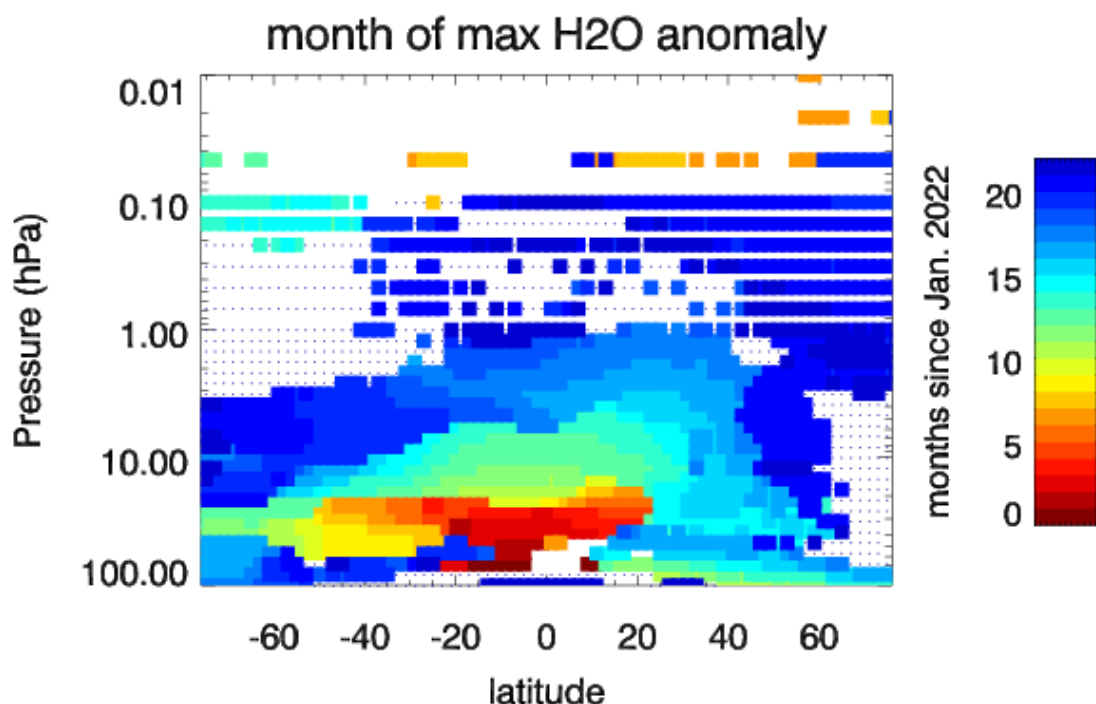
289
 290 **Figure 6-** Daily anomalies in 100 hPa temperature from 10°S-10°N from MERRA2 relative to a
 291 1980-present average. The blue line is from a 365-day smoothing.

292 In Figure 7 we show a measure of the rate of spread of the H₂O plume. As in Figure 1, a zonal
 293 monthly median has been calculated from monthly MLS data in 2° latitude bins, and a monthly
 294 climatology has been subtracted. Figure 7 then shows the month in which the H₂O mixing ratio
 295 anomaly at each latitude and pressure reaches a maximum value. The unprecedented global
 296 effect of the Hunga Tonga eruption is apparent in that, for nearly every location up to 0.1 hPa,
 297 the monthly maximum zonal median H₂O anomaly has occurred in the months since January
 298 2022. This statement is also true for the maximum absolute H₂O mixing ratio.

299 During the first two months after the eruption, the increased H₂O in the plume causes sufficient
 300 radiative cooling and to significantly perturb the vertical velocity (Randel et al. 2023; Niemeier
 301 et al., 2023). Niemeier et al. (2023) show that this velocity perturbation decreases in subsequent
 302 months. There is also gradual CH₄ oxidation that occurs in the stratosphere which increases H₂O
 303 mixing ratios. H₂O is therefore not a perfectly non-interacting tracer. Nevertheless, especially in

304 the upper stratosphere and mesosphere where the radiative cooling effects are small, Figure 7 can
305 provide timescales for the transport of a tracer from the Hunga Tonga injection site at ~20-30
306 hPa and 20.5°S. Qualitatively, the timescale at which the month of maximum anomaly rises in
307 the tropics from 10 hPa to 1 hPa is comparable to the residual vertical velocity and the change in
308 modal age-of-air for the tropical pipe region in the Goddard Earth Observing System Chemistry-
309 Climate Model shown in Li et al. (2012)

310 Figure 7 shows that the plume spread quickly in the tropics in the low and mid-stratosphere, as
311 was previously noted by Schoeberl et al. (2023). It was first clearly observed in early April by
312 WVMS measurements at Mauna Loa (19.5°N) at 28 km, using a non-standard retrieval technique
313 that provided sensitivity in the mid-stratosphere (Nedoluha et al., 2023a). But the ascent into the
314 mid-stratosphere took much longer, with the maximum H₂O anomalies in the mid-stratosphere in
315 the tropics not occurring until almost a year after the eruption.



316
317 **Figure 7-** The number of months after the eruption of Hunga Tonga that the zonal median MLS
318 H₂O anomaly reached its maximum value. Small dots indicate that the maximum occurred in the
319 last month shown (November 2023). Results are shown for all MLS pressure levels from 100 to
320 0.01 hPa and in 2 degree latitude increments. Regions with no symbol (primarily in the upper
321 mesosphere) indicate that the maximum H₂O anomaly occurred before January 2022.

322 The asymmetry in the evolution of the SH and NH tropics, shown in Figure 2, is also apparent in
323 Figure 7. There is a maximum in SH tropical upper stratosphere at 20S at 1.8 hPa in March
324 2023, but not until September does the maximum reach 1 hPa. By contrast, the maximum in the
325 NH tropics at 1.8 hPa occurs in May, but it reaches 1 hPa and enters the mesosphere soon
326 thereafter.

327 There are at least two regions where the month of maximum H₂O occurs during this time period,
328 but is unrelated to the Hunga Tonga plume. The maxima in H₂O in the SH upper mesosphere in
329 August 2022, and at the highest northern latitudes in February and March 2022, are primarily
330 caused by unusual dynamical conditions, as is evidenced by unusually low CO mixing ratios, as
331 was shown in N23.

332 **5. Summary**

333 While the high mesospheric H₂O mixing ratios observed in 2022 were unprecedented, the
334 increase observed in 2023 was much larger and more widespread. By October 2023 large
335 (>1ppmv) anomalies were observed throughout the lower mesosphere by Aura MLS and by three
336 WVMS instruments. At Table Mountain all WVMS H₂O measurements at 54 km since June
337 2023, and all of the measurements from Mauna Loa since the resumption of measurements in
338 September 2023, show larger mixing ratios than any previous measurements. At 70 km several
339 WVMS measurements in the last few months from Table Mountain and Mauna Loa show the
340 largest anomalies ever measured at these sites.

341 The MLS measurements allow for the tracking of the spread of the Hunga Tonga plume
342 throughout the middle atmosphere, and maximum H₂O anomaly values have occurred
343 throughout almost all of the stratosphere and lower mesosphere since the eruption. These
344 measurements also show that, as the water vapor spread, the total mass anomaly in the
345 stratosphere and lower mesosphere (82 hPa to 0.1 hPa) remained nearly constant, so that, 22
346 months after the eruption, almost all of the water injected into the middle atmosphere during the
347 Hunga Tonga eruption remains in the middle atmosphere.

348 **6. Acknowledgments**

349 We thank G. Rose, M. Kotkamp, M. Brewer, J. Robinson, and P. Wang for their efforts to
350 maintain and calibrate the WVMS instruments at Mauna Loa, Table Mountain, and Lauder. This
351 work was supported by the NASA Earth Sciences Division Upper Atmosphere Research
352 Program and by the Office of Naval Research. Work at the Jet Propulsion Laboratory, California
353 Institute of Technology, was carried out under a contract with the National Aeronautics and
354 Space Administration. We thank M. Heney for making the daily GMA:GEOS5 temperature data
355 at each site available in a convenient form.

356 **7. Data Availability Statement**

357 WVMS weekly retrievals are available on the NDACC data server at [https://www-](https://www-air.larc.nasa.gov/missions/ndacc/data.html#)
358 [air.larc.nasa.gov/missions/ndacc/data.html#](https://www-air.larc.nasa.gov/missions/ndacc/data.html#). MLS v5 data are available at
359 https://disc.gsfc.nasa.gov/datasets?page=1&keywords=ML2H2O_005. HALOE v19 data are
360 available at disc.gsfc.nasa.gov/datasets?keywords=HALOE. GEOS temperature data are
361 available at https://gmao.gsfc.nasa.gov/GMAO_products/. Lyman-alpha timeseries based on
362 work of Machol et al. (2019).

363 **8. References**

364 Bernath, P.F., et al.,: Atmospheric Chemistry Experiment (ACE): Mission overview (2005),
365 Geophys. Res. Lett., 32, L15S01, <https://doi.org/10.1029/2005GL022386>, 2005.

366 Carr, J. L., Horváth, Á., Wu, D. L., & Friberg, M. D. (2022). Stereo plume height and motion
367 retrievals for the record-setting Hunga Tonga-Hunga Ha'apai eruption of 15 January 2022.
368 Geophysical Research Letters, 49, e2022GL098131. <https://doi.org/10.1029/2022GL098131>

369 Dessler, A. E., M. R. Schoeberl, T. Wang, S.M. Davis, K. H. Rosenlof, and J.-P. Vernier (2014),
370 Variations of stratospheric water vapor over the past three decades, J. Geophys. Res. Atmos.,
371 119, 12,588–12,598, doi:10.1002/2014JD021712.

372 Evans, S. J., Toumi, R., Harries, J. E., Chipperfield, M. P., & Russell, J. M. (1998). Trends in
373 stratospheric humidity and the sensitivity of ozone to these trends. Journal of Geophysical
374 Research, 103(D8), 8715–8725. <https://doi.org/10.1029/98JD00265>

375 Fleming, E. L., Newman, P. A., Liang, Q., & Oman, L. D. (2024). Stratospheric temperature and
376 ozone impacts of the Hunga Tonga-Hunga Ha'apai water vapor injection. Journal of Geophysical
377 Research: Atmospheres, 129, e2023JD039298. <https://doi.org/10.1029/2023JD039298>

378 Gomez, R. M., G. E. Nedoluha, H. L. Neal, and I. S. McDermid, The fourth generation Water
379 Vapor Millimeter-Wave Spectrometer, Radio Sci., 47,RS1010, doi:10.1029/2011RS004778,
380 (2012).

381 Khaykin, S., Podglajen, A., Ploeger, F., Grooß, J. U., Tencé, F., Bekki, S., et al. (2022). Global
382 perturbation of stratospheric water and aerosol burden by Hunga eruption. Communications
383 Earth & Environment, 3(1), 316. <https://doi.org/10.1038/s43247-022-00652-x>

384 Laboratory for Atmospheric and Space Physics. (2005). LASP Interactive Solar Irradiance
385 Datacenter. Laboratory for Atmospheric and Space Physics. [https://doi.org/10.25980/L27Z-](https://doi.org/10.25980/L27Z-XD34)
386 [XD34](https://doi.org/10.25980/L27Z-XD34)

387 Li, F., D.W. Waugh, A. R. Douglass, P. A. Newman, S. E. Strahan, J. Ma, J. E. Nielsen, and Q.
388 Liang (2012), Long-term changes in stratospheric age spectra in the 21st century in the Goddard
389 Earth Observing System Chemistry-Climate Model (GEOSCCM), J. Geophys. Res., 117,
390 D20119, doi:10.1029/2012JD017905.

391 Livesey, N. J., et al. (2021), Investigation and amelioration of long-term instrumental drifts in
392 water vapor and nitrous oxide measurements from the Aura Microwave Limb Sounder (MLS)
393 and their implications for studies of variability and trends, Atmos. Chem. Phys., 21, 15409–
394 15430, 2021.

395 Machol, J., Snow, M., Woodraska, D., Woods, T., Viereck, R., & Coddington, O. (2019). An
396 improved lyman-alpha composite. Earth and Space Science, 6, 2263–2272.
397 <https://doi.org/10.1029/2019EA000648>

398 Millán, L., Santee, M. L., Lambert, A., Livesey, N. J., Werner, F., Schwartz, M. J., et al. (2022).
399 The Hunga Tonga-Hunga Ha'apai Hydration of the Stratosphere. Geophysical Research Letters,
400 49, e2022GL099381. <https://doi.org/10.1029/2022GL099381>.

401 Nedoluha, G. E., Bevilacqua, R. M., Gomez, R. M., Siskind, D. E., Hicks, B. C., Russell, J. M.,
402 III, & Connor, B. J. (1998a). Increases in middle atmospheric water vapor as observed by

403 HALOE and the ground-based Water Vapor Millimeter-wave Spectrometer from 1991–1997.
404 Journal of Geophysical Research, 103(D3), 3531–3542. <https://doi.org/10.1029/97jd03282>

405 Nedoluha, G. E., et al., Changes in upper stratospheric CH₄ and NO₂ as measured by HALOE
406 and implications for changes in transport, Geophys. Res. Lett., 25, 987–990, 1998b.

407 Nedoluha, G. E., R. M. Bevilacqua, R. M. Gomez, B. C. Hicks, J. M. Russell III, and B. J.
408 Connor, An evaluation of trends in middle atmospheric water vapor as measured by HALOE,
409 WVMS, and POAM, J. Geophys. Res., 108(D13), 4391, doi:10.1029/2002JD003332, 2003.

410 Nedoluha, G. E., R. M. Gomez, B. C. Hicks, J. E. Wrotny, C. Boone, and A. Lambert (2009),
411 Water vapor measurements in the mesosphere from Mauna Loa over solar cycle 23, J. Geophys.
412 Res., 114, D23303, doi:10.1029/2009JD012504.

413 Nedoluha, Gerald E., R. Michael Gomez, Ian Boyd, Helen Neal, Douglas R. Allen, David
414 Siskind, Alyn Lambert, and Nathaniel J. Livesey, (2022). Measurements of Mesospheric Water
415 Vapor from 1992 to 2021 at three stations from the Network for the Detection of Atmospheric
416 Composition Change, Journal of Geophysical Research: Atmospheres, 127, e2022JD037227.
417 <https://doi.org/10.1029/2022JD037227>

418 Nedoluha, Gerald E., R. Michael Gomez, Ian Boyd, Helen Neal, Douglas R. Allen, Alyn
419 Lambert, and Nathaniel J. Livesey, (2023a). Measurements of stratospheric water vapor at
420 Mauna Loa and the effect of the Hunga Tonga eruption. Journal of Geophysical Research:
421 Atmospheres, 128, e2022JD038100. <https://doi.org/10.1029/2022JD038100>

422 Nedoluha, G. E., et al. (2023b). Mesospheric water vapor in 2022. Journal of Geophysical
423 Research: Atmospheres, 128, e2023JD039196. <https://doi.org/10.1029/2023JD039196>

424 Niemeier, U., Wallis, S., Timmreck, C., van Pham, T., & von Savigny, C. (2023). How the
425 Hunga Tonga—Hunga Ha'apai water vapor cloud impacts its transport through the stratosphere:
426 Dynamical and radiative effects. Geophysical Research Letters, 50, e2023GL106482.
427 <https://doi.org/10.1029/2023GL106482>

428 Randel, W. J., et al., (1998). Seasonal Cycles and QBO Variations in Stratospheric CH₄ and H₂O
429 Observed in UARS HALOE Data, Journal of Atmospheric Sciences, DOI10.1175/1520-
430 0469(1998)055<0163:SCAQVI>2.0.CO;2

431 Russell, J. M., Gordley, L. L., Park, J. H., Drayson, S. R., Hesketh, W. D., Cicerone, R. J., et al.
432 (1993). The Halogen Occultation Experiment, Journal of Geophysical Research, 98(D6), 10777–
433 10797. <https://doi.org/10.1029/93JD00799>

434 Randel, W. J., Johnston, B. R., Braun, J. J., Sokolovskiy, S., Vömel, H., Podglajen, A., & Legras,
435 B. (2023). Stratospheric water vapor from the Hunga Tonga Hunga Ha'apai volcanic eruption
436 deduced from COSMIC-2 radio occultation. Remote Sensing, 15(8), 2167.
437 <https://doi.org/10.3390/rs15082167>

- 438 Schoeberl, M. R., Wang, Y., Ueyama, R., Taha, G., Jensen, E., & Yu, W. (2022). Analysis and
439 impact of the Hunga Tonga-Hunga Ha'apai stratospheric water vapor plume. *Geophysical*
440 *Research Letters*, 49, e2022GL100248. <https://doi.org/10.1029/2022GL100248>
- 441 Teniente, J., Gomez, R. M., Maestrojuan, I., Rebollo, A., Gonzalo, R., Del-Río, C. “Corrugated
442 Horn Antenna Noise Temperature Characterization for the NRL Water Vapor Millimeter-Wave
443 Spectrometer Project”, *Proceedings of the 5th European Conference on Antennas and*
444 *Propagation*, 934 - 938, (EuCAP 2011)
- 445 Wilmouth, D. M., et al., Impact of the Hunga Tonga volcanic eruption on stratospheric
446 composition, *PNAS*, <https://doi.org/10.1073/pnas.2301994120>.
- 447 Xu, J., Li, D., Bai, Z., Tao, M., & Bian, J. (2022). Large amounts of water vapor were injected
448 into the stratosphere by the Hunga Tonga–Hunga Ha'apai volcano eruption. *Atmosphere*, 13(6),
449 912. <https://doi.org/10.3390/atmos13060912>